EUROPEAN SPALLATION SOURCE

Neutron Sources

Christine Darve

African School of Fundamental Physics and its Applications

August 20, 2014

Outline

- Neutrons properties and their interactions
- How to generate intense neutron beams using high power proton linear accelerator: The example of the ESS

for further reading

- Applications using Neutrons

General Applications

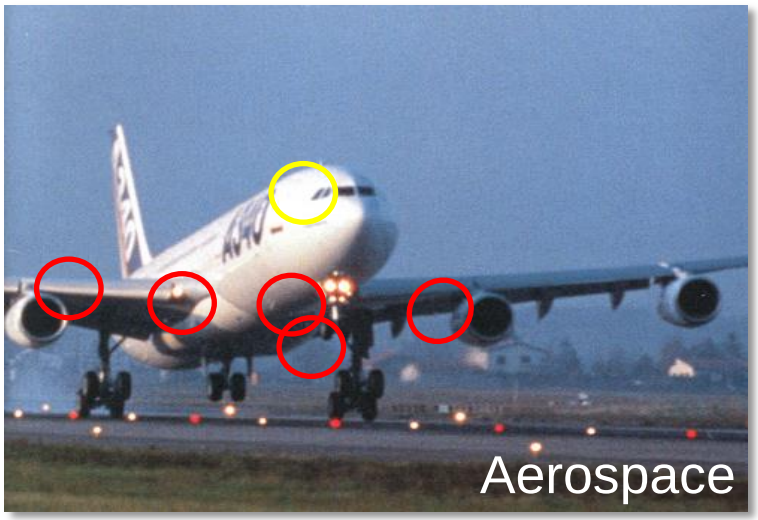

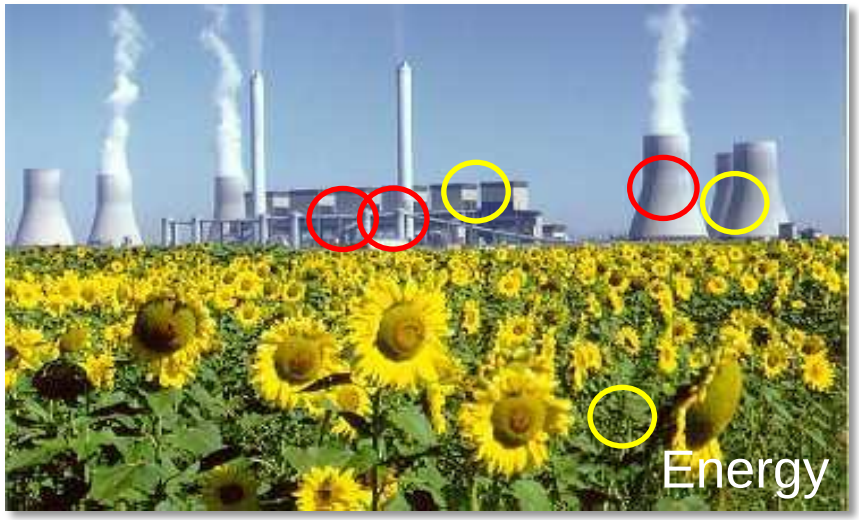

Neutron Coherency Length

PRL **100,** 250404 (2008) PHYSICAL REVIEW LETTERS week ending 27 JUNE 2008

Measurements of the Vertical Coherence Length in Neutron Interferometry

D. A. Pushin,[1,*] M. Arif,[2] M. G. Huber,[3] and D. G. Cory[1]

[1]*Department of Nuclear Science and Engineering, Massachusetts Institute of Technology, Cambridge, Massachusetts, USA*
[2]*National Institute of Standards and Technology, Gaithersburg, Maryland, USA*
[3]*Department of Physics, Tulane University, New Orleans, Louisiana, USA*

(Received 19 March 2008; published 26 June 2008)

The study and use of macroscopic quantum coherence requires long coherence lengths. Here we describe an approach to measuring the vertical coherence length in neutron interferometry, along with improvements to the NIST interferometer that led to a measured coherence length of 790 Å. The measurement is based on introducing a path separation and measuring the loss in contrast as this separation is increased. The measured coherence length is consistent with the momentum distribution of the neutron beam. Finally, we demonstrate that the loss in contrast with beam displacement in one leg of the interferometer can be recovered by introducing a corresponding displacement in the second leg.

DOI: 10.1103/PhysRevLett.100.250404 PACS numbers: 03.75.Dg, 03.65.−w, 42.50.−p

Small-Angle (SANS/SAXS)

EUROPEAN SPALLATION SOURCE

Velocity selector | Collimation

- Polymers and colloids, e.g.
  - Micelles
  - Dendrimers
  - Liquid crystals
  - Gels
  - Reaction kinetics of m
- Materials Science
  - Phase separation in all
  - Morphologies of supe
  - Micro-porosity in c
  - Interfaces and surf
- Biological macromolecul
  - Size and shape of and of macromolecu
  - Bio-membranes
  - Drug vectors
- Magnetism
  - Magnetic correlati
  - Flux line lattices in

D22 at www.ill.eu

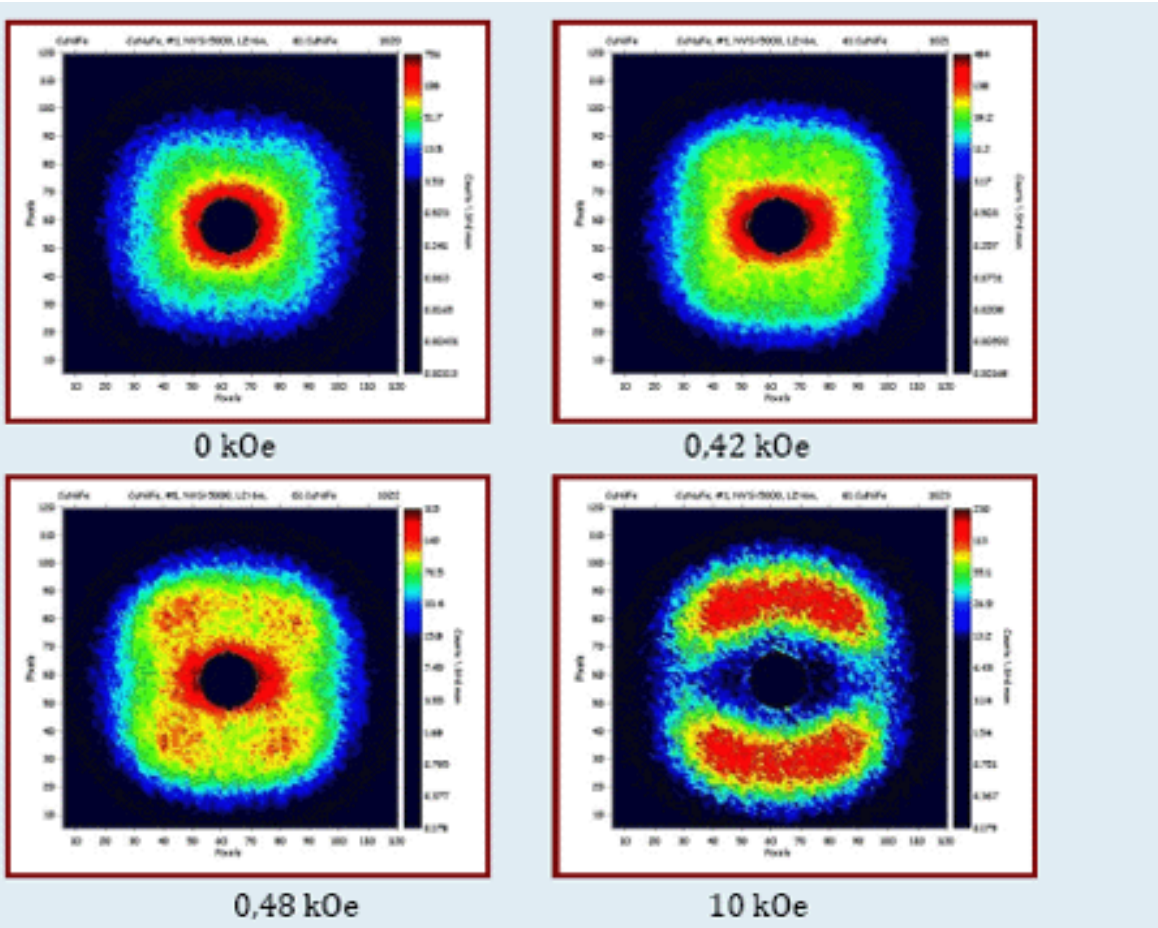

Figure 32. Sequence of two-dimensional corrected SANS pattern from magnetic sample of Cu(NiFe) metal-alloy in the external magnetic field

calculated scattering curve corresponds to the scattering from four independent Gaussian partici as indicated by D1-D4. b) Fit results to the measured scattering curve shown in a). Fitting using 4 independent Gaussian distributions (D1-D4). The corresponding errors are indicated by thin lines.

Polymers

Macromolecules
ARTICLE

Macromolecules **2010**, *43*, 9837–9847
DOI: 10.1021/ma101898c

sites

Quasielastic Neutron Scattering Study on the Dynamics of Poly(alkylene oxide)s

C. Gerstl,[†,‡] G. J. Schneider,[*,‡] A. Fu
J. Allgaier,[†] D. Richter,[†,‡] J. Colmene

[†]Jülich Centre for Neutron Science (JCNS 1)
D−52425 Jülich, Germany
[‡]Jülich Centre for Neutron Science (JCNS 1),
[#]Institut Laue−Langevin, BP 156, 38042 Gren
[§]Laboratoire Charles Coulomb, UMR 5221, C
[∥]Centro de Física de Materiales (CSIC, UPV/
E-20018 San Sebastián, Spain
[⊥]Departamento de Física de Materiales (UPV/
[○]Donostia International Physics Center, Pase

ABSTRACT: By means of quasielastic neu
investigated the hydrogen dynamics in poly(
with different side-chain lengths at temper
above the glass-transition. The combinatio
different spectrometers (a time-of-flight
instruments) has allowed covering almost 4
time—from the ps to ns range—with spatia
evidence the simultaneous occurrence of
side-group motions at low temperatures and
(segmental) dynamics at high temperatures.
of the side groups show (i) stretching of
(ii) associated activation energies similar to th
cooperative bond rotations of polyethylene,
that increase with increasing temperature. Co
presents (i) the same spectral shape, (ii) slo
behavior. For comparison, we also report o
in the same temperature range, that show ev
with intrinsic dynamic heterogeneities bet
confinement effects.

Introduction

AS

8218 *Macromolecules* **2010**, *43*, 8218–8232
DOI: 10.1021/ma101235j

Macromolecules
ARTICLE

In Situ and Time-Resolved Small-Angle Neutron Scattering Observation of Star Polymer Formation via Arm-Linking Reaction in Ruthenium-Catalyzed Living Radical Polymerization[1]

Takaya Terashima,[*,†] Ryuhei Motokawa,[*,‡] Satoshi Koizumi,[*,‡] Mitsuo Sawamoto,[*,†] Masami Kamigaito,[§] Tsuyoshi Ando,[†,∥] and Takeji Hashimoto[‡]

[†]*Department of Polymer Chemistry, Graduate School of Engineering, Kyoto University, Katsura, Nishikyo-ku, Kyoto 615-8510, Japan,* [‡]*Research Group for Soft Matter & Neutron Scattering, Advanced Science Research Center, JAEA, Ibaraki 319-1195, Japan, and* [§]*Department of Applied Chemistry, Graduate School of Engineering, Nagoya University, Furo-cho, Chikusa-ku, Nagoya 464-8603, Japan.* [∥]*Present address: Graduate School of Material Science, Nara Institute of Science and Technology, 8916-5 Takayama-cho, Ikoma, Nara 630-0192, Japan*

Received June 2, 2010; Revised Manuscript Received August 12, 2010

ABSTRACT: *In situ* and time-resolved small-angle neutron scattering (SANS) was employed for the elucidation of star polymer formation mechanism via linking reaction of living linear polymers in ruthenium-catalyzed living radical polymerization. Here, methyl methacrylate (MMA) was first polymerized with R−Cl/$RuCl_2(PPh_3)_3$/tribuylamine (n-Bu_3N) initiating system, followed by the addition of ethylene glycol dimethacrylate (EGDMA: **3**) as a linking agent. After the *in situ* addition of a small amount of **3** to living linear PMMA, the SANS analysis revealed the following three steps: (process II-1) formation of block copolymers (**4**) and competitive formation of the small star polymers via the linking reaction of **4** and **4**; (process II-2) star−star linking of the small star polymers into star polymers and putting **4** into the core of the star polymers, leading to formation of the microgel-core star polymers; (process II-3) growth of the microgel-core star polymers (**5**) via placement of **4** into the microgel-core star polymers. Furthermore, the SANS profiles, obtained as a function of polymerization time, were quantitatively analyzed with a core−shell spherical model in order to determine the microstructures of the star polymers: The final reaction product had an average radius of microgel-core (∼1 nm), and average arm numbers $N \sim 17$.

Contrast Variation

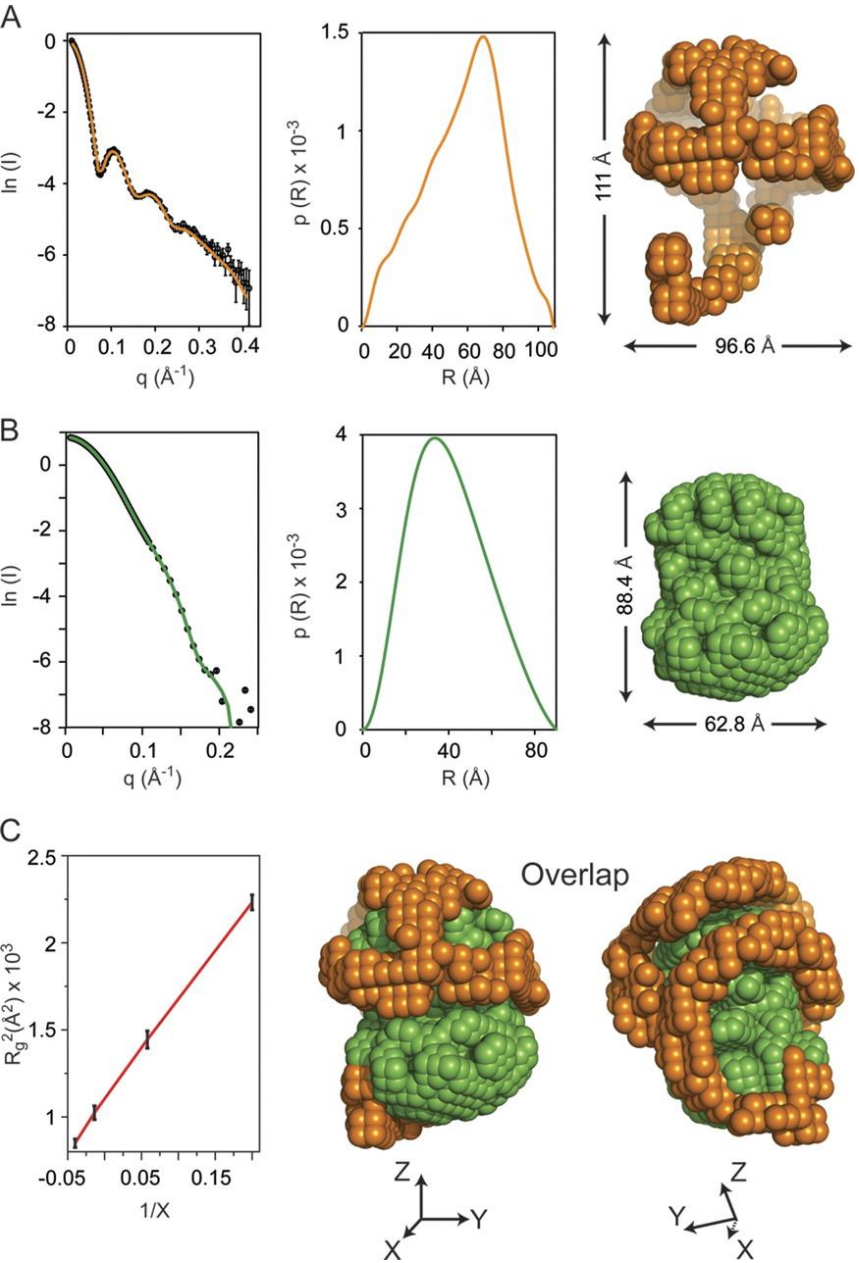

Spherical high density lipoprotein (sHDL), a key player in reverse cholesterol transport and the most abundant form of HDL, is associated with cardiovascular diseases.
Small angle neutron scattering with contrast variation was used to determine the solution structure of protein and lipid components of reconstituted sHDL. Apolipoprotein A1, the major protein of sHDL, forms a hollow structure that cradles a central compact lipid core. Three apoA1 chains are arranged within the low resolution structure of the protein component as one of three possible global architectures: (i) a helical dimer with a hairpin (HdHp), (ii) three hairpins (3Hp), or (iii) an integrated trimer (iT) in which the three apoA1 monomers mutually associate over a portion of the sHDL surface. Cross-linking and mass spectrometry analyses help to discriminate among the three molecular models and are most consistent with the HdHp overall architecture of apoA1 within sHDL

Courtesy Z. Wu (Cleveland) 10.1074/jbc.M110.209130

Contents lists available at ScienceDirect

Food Research International

journal homepage: www.elsevier.com/locate/foodres

Review

Nanocomposites for food packaging applications

Henriette M.C. de Azeredo*

Embrapa Tropical Agroindustry, R. Dra. Sara Mesquita, 2270, Fortaleza, CE, CEP 60511-110, Brazil

ARTICLE INFO

Article history:
Received 3 January 2009
Accepted 30 March 2009

Keywords:
Nanotechnology
Biodegradable polymers
Whiskers
Nanofillers

ABSTRA

Most materials
lems. Several b
However, the u
properties, whi
reinforced mate
dimensions. Th
posites. Nanopa
favors the fille
forcements, na
activity, enzym
ied for use in fo

Contents

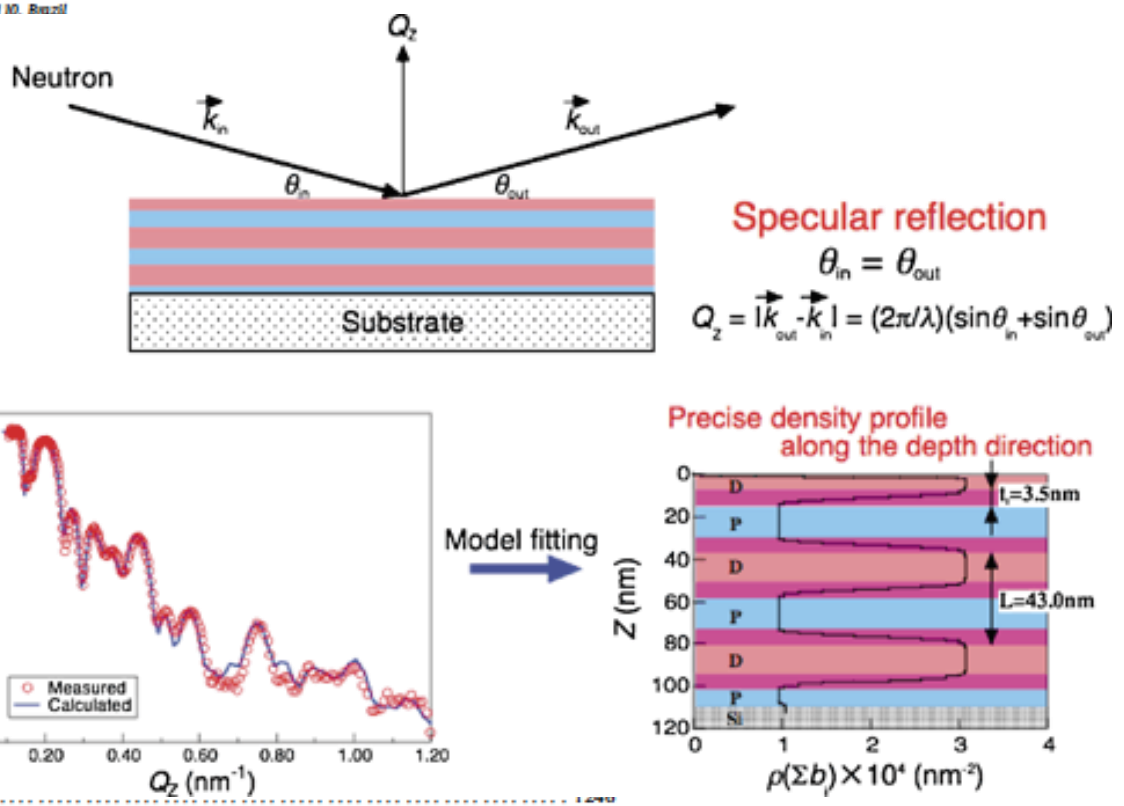

Fuel Cells & Hydrogen Economy

EUROPEAN SPALLATION SOURCE

Nuclear Instruments and Methods in Physics Research A 605 (2009) 115–118

Contents lists available at ScienceDirect

Nuclear Instruments and Methods in Physics Research A

journal homepage: www.elsevier.com/locate/nima

Neutron radiography characterization of an operating proton exchange membrane fuel cell with localized current distribution measurements

J.J. Gagliardo *, J.P. Owejan, T.A. Trabold, T.W. Tighe

General Motors Corporation, Fuel Cell Research Laboratory, Honeoye Falls, NY 14472-0603, USA

ARTICLE INFO

Available online 5 February 2009

Keywords:
Neutron radiography
Fuel cell
Proton exchange membrane
Water management
Current distribution

ABSTRACT

Neutron radiography has proven to be a powerful tool to study and understand the effects of liquid water in an operating fuel cell. In the present work, this experimental method is coupled with locally resolved current and ohmic resistance measurements, giving additional insight into water management and fuel cell performance under a variety of conditions. The effects of varying the inlet humidification level and the current density of the 50 cm^2 cell are studied by simultaneously monitoring electrochemical performance with a 10×10 matrix of current sensors, and liquid water volumes are measured using the National Institute of Standards and Technology (NIST) neutron imaging facility. A counter flow, straight channel proton exchange membrane (PEM) fuel cell is used to demonstrate localized performance loss corresponds to water-filled channels that impede gas transport to the catalyst layer, thereby creating an area that has low current density. Furthermore, certain operating conditions causing excess water accumulation in the channels can result in localized proton resistance increase, a result that can only be accurately observed with combined radiography and distributed electrochemical measurements.

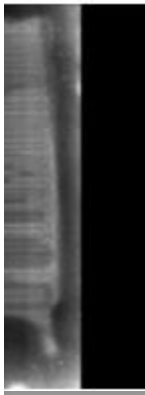

Solar Cells

THE JOURNAL OF CHEMICAL PHYSICS 133, 074902 (2010)

Phase-sensitive neutron reflectometry measurements applied in the study of photovoltaic films

J. W. Kiel,[1,2] M. E. Mackay,[2,a)] B. J. Kirby,[3] B. B. Maranville,[3] and C. F. Majkrzak[3,a)]
[1]*Department of Chemical Engineering and Materials Science, Michigan State University, East Lansing, Michigan 48824, USA*
[2]*Department of Materials Science and Engineering, The University of Delaware, Newark, Delaware 19716, USA*
[3]*National Institute of Standards and Technology Center for Neutron Scattering, Gaithersburg, Maryland 20899, USA*

(Received 4 May 2010; accepted 5 July 2010; published online 20 August 2010)

Due to low charge carrier mobilities in polymer-based solar cells, device performance is dictated by the nanoscale morphology of the active layer components. However, their morphological details are notoriously difficult to distinguish due to the low electron contrast difference between the components. Phase-sensitive neutron reflectivity (PSNR) is uniquely suited to characterize these systems due to the large, natural scattering length density difference between two common device materials, poly(3-hexylthiophene) and [6,6]-phenyl-C61-butyric acid methyl ester (PCBM). Using PSNR we find a high concentration of PCBM at the substrate and near but not at the air interface. Herein we discuss the method of applying PSNR to polymer-based solar cells, the results obtained, and an evaluation of its effectiveness. © *2010 American Institute of Physics*.

Courtesy: STFC, UK

Hydrogen Storage

EUROPEAN SPALLATION SOURCE

Hydrogen Storage in a Microporous Metal−Organic Framework with Exposed Mn^{2+} Coordination Sites

Mircea Dincă,[†] Anne Dailly,[‡,⊥] Yun Liu,[§,∥] Craig M. Brown,[§,#] Dan. A. Neumann,[§] and Jeffrey R. Long*[,†]

Contribution from the Department of Chemistry, University of California, Berkeley, California 94720, Chemical and Environmental Sciences Laboratory, General Motors Corporation, Warren, Michigan 48090, College of Engineering, Purdue University, West Lafayette, Indiana 47907, Center for Neutron Research, National Institute of Standards and Technology, Gaithersburg, Maryland 20899, Department of Materials Science and Engineering, University of Maryland, College Park, Maryland 20742, and Indiana Universit Bloomington, Indiana 47408

Received August 5, 2006; E-mail: jrlong@berkeley.e

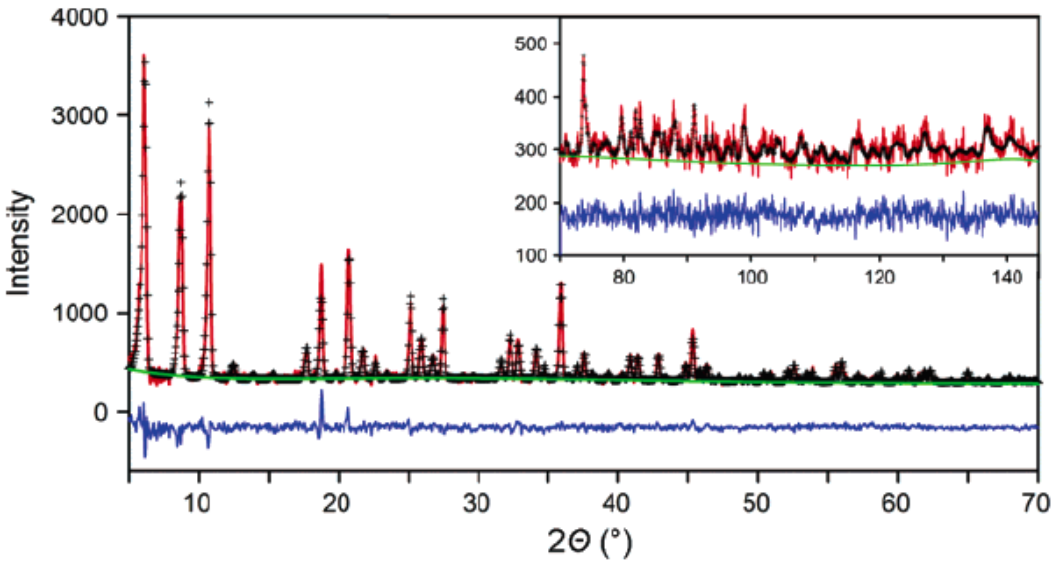

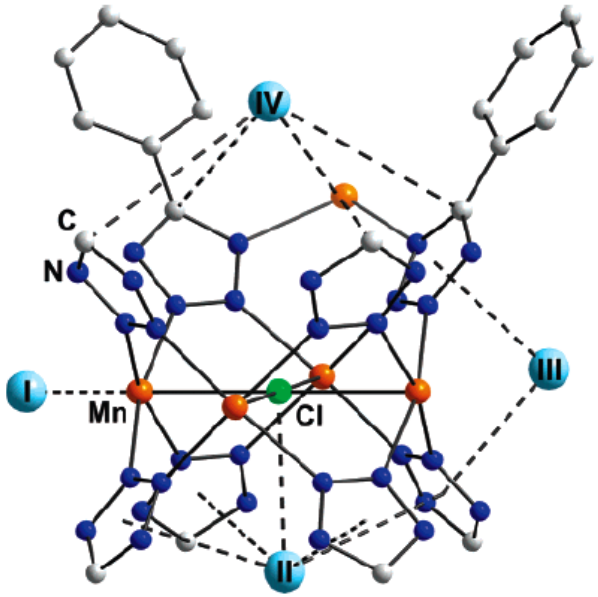

Figure 7. Initial D_2 adsorption sites within **1m′**. Light blue spheres represent D_2 centroids, while the transparent orange sphere shows the position of a partially occupied, extraframework Mn^{2+} ion site. Hydrogen atoms and methanol molecules are omitted for clarity.

YBCO

- $YBa_2Cu_3O_7$, $YBa_2Cu_3O_{7-x}$
- High-Tc superconductor
- x=0.07, Tc=93K most efficient

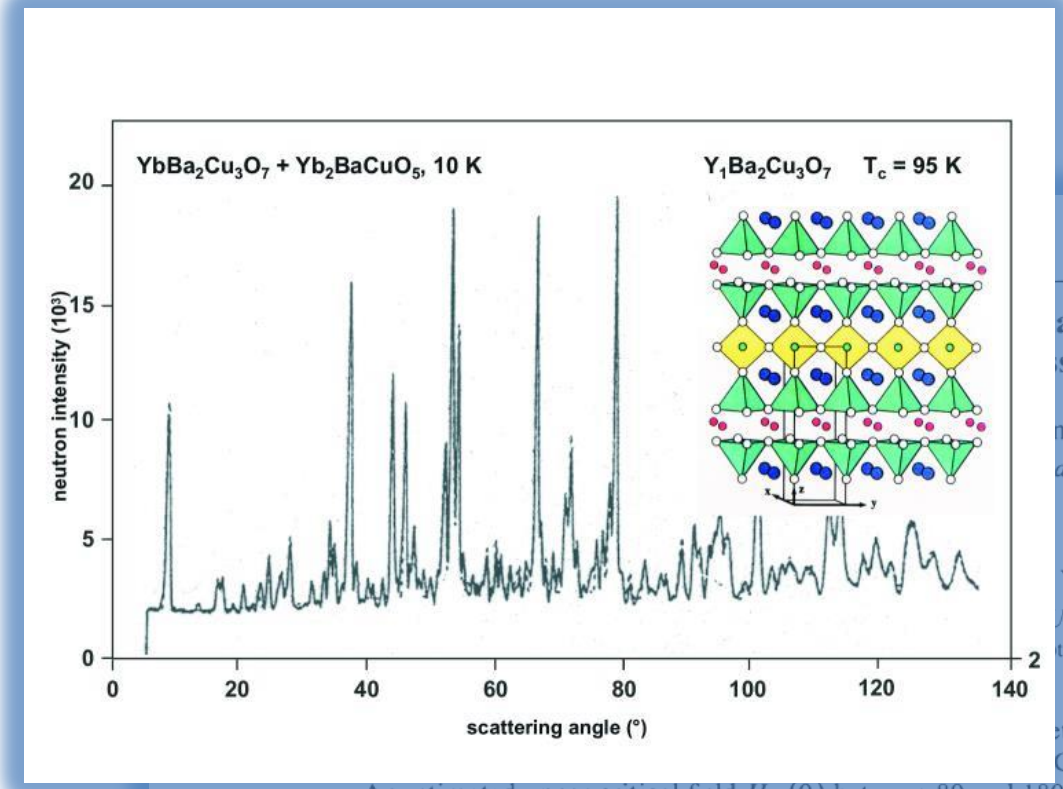

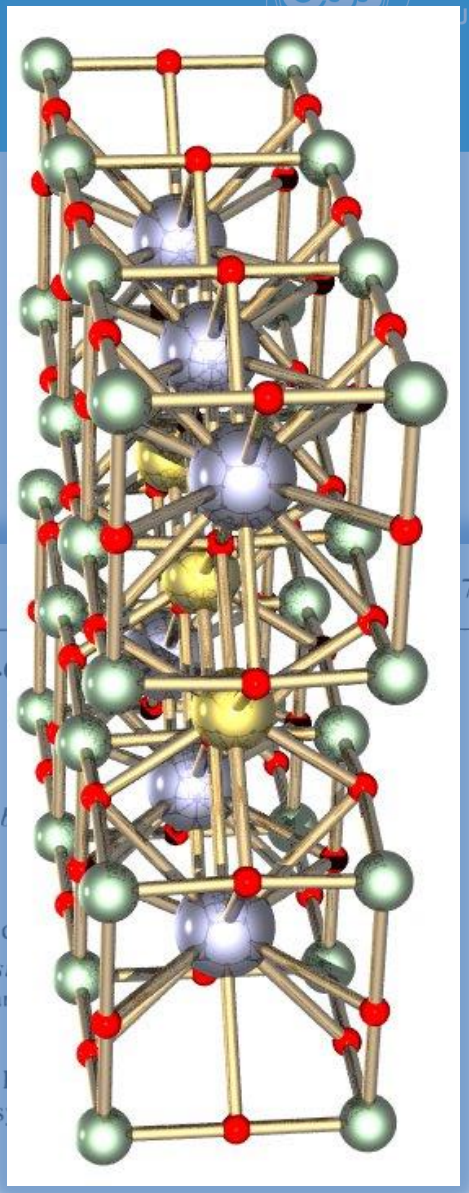

LETTERS

ase Y-Ba-Cu-
ssure

nd C. J. Torng
a, Huntsville, Alab

Y. Q. Wang, and
University of Hous
t received 18 Februa

tween 80 and 93
Cu-O compound s

An estimated upper critical field $H_{c2}(0)$ between 80 and 180 T was obtained.

PACS numbers: 74.70.Ya

Forefront of Science

EUROPEAN SPALLATION SOURCE

letters to nature

Superconductivity in the non-oxide perovskite $MgCNi_3$

T. He*, Q. Huang†, A. P. Ramirez‡, Y. Wang§, K. A. Regan*, N. Rogado*, M. A. Hayward*, M. K. Haas*, J. S. Slusky*, K. Inumara*, H. W. Zandbergen*, N. P. Ong§ & R. J. Cava*

** Department of Chemistry and Princeton Materials Institute; § Department of Physics, Princeton University, Princeton, New Jersey, USA*
† Department of Materials and Nuclear Engineering, University of Maryland, College Park, Maryland; and NIST Center for Neutron Research, Gaithersburg, Maryland, USA
‡ Condensed Matter and Thermal Physics Group, Los Alamos National Laboratory, Los Alamos, New Mexico, USA

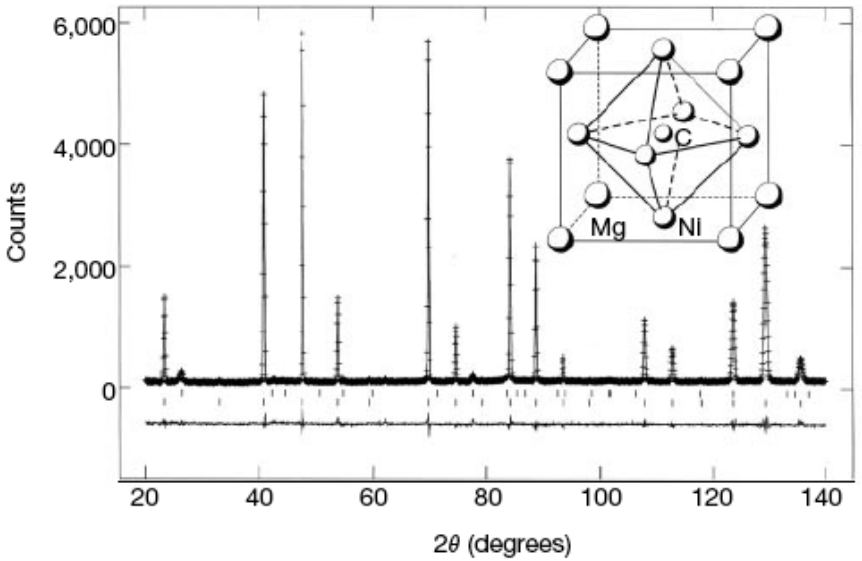

Figure 1 The powder neutron diffraction pattern at ambient temperature for the sample of nominal composition $MgC_{1.25}Ni_3$ and the perovskite crystal structure for the superconducting compound $MgCNi_3$ (inset). Neutrons of wavelength 1.5402 Å were employed (Cu 311 monochromator), with collimators of 15′, 20′ and 7′ of arc before and after the monochromator, and after the sample, respectively. The neutron scattering lengths employed in the structure refinement were 0.538, 0.665 and 1.030 (cm^{-12}) for Mg, C and Ni, respectively. Data are shown as crosses, and the difference plot between model and data shown directly below. The vertical lines (bottom) show the Bragg peak positions for the $MgCNi_3$ phase. The sample contains 2 wt% graphite (about 25 mol.%) in agreement with the nominal composition. Positions of the graphite peaks are shown as vertical lines above those for $MgCNi_3$. The refinement agreement, weighted profile agreement, and χ^2 values obtained were $R = 5.14\%$, $R_w = 6.39\%$ and $\chi^2 = 1.258$, indicating the high quality of the structural model.

Buckminster Fullerenes

High resolution neutron powder diffraction: a case study of the structure of C_{60}

By W. I. F. David[1], R. M. Ibberson[1] and T. Matsuo[2]

[1] *ISIS Science Division, Rutherford Appleton Laboratory, Chilton, Didcot, Oxon OX11 0QX, U.K.*

[2] *Department of Chemistry and Microcalorimetry Research Centre, Faculty of Science, Osaka University, Toyonaka 560, Japan*

High resolution time-of-flight neutron powder diffraction has been used to determine the detailed structure of C_{60} as a function of temperature. Rapid data collection coupled with high resolution has enabled subtle aspects of the 86 K orientational glass transition and precursor effects of the 260 K order–disorder transition to be observed. This surveying capability complements traditional single crystal methods. The power of the Rietveld method of profile refinement is demonstrated in the elucidation of the detailed crystal structure of the orientationally-ordered low temperature phase and in the evaluation of the departure from isotropic scattering of the C_{60} molecule in the disordered high temperature phase. The counter-intuitive success in obtaining high-order cubic-harmonic coefficients, albeit to poorer precision than single crystal X-ray measurements, confirms the efficacy of the Rietveld profile refinement method. The collapse of three dimensions of diffraction information on to the one dimension of a high resolution powder diffraction pattern can still lead to an impressive amount of structural information that substantiates the assertion made by W. H. Bragg

> 'the second method [powder diffraction], first used independently by Debye and Hull, can be used when the crystal is in powder, and can, therefore be employed when no single crystal can be obtained of sufficient size. All the spectra of the different planes are thrown together on the same diagram or photograph, and must be disentangled. This is not as difficult as it may seem ...'.

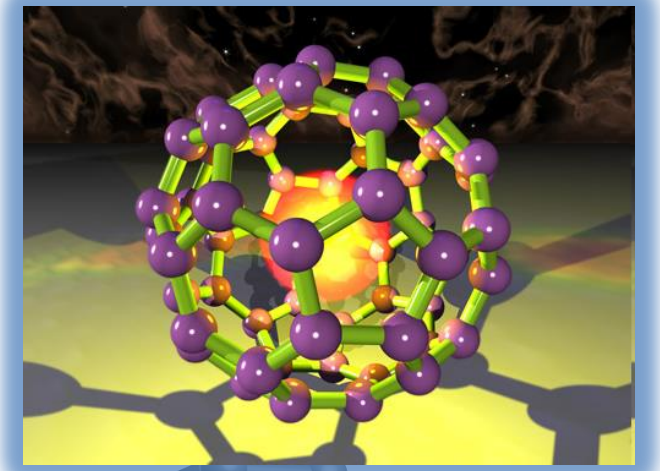

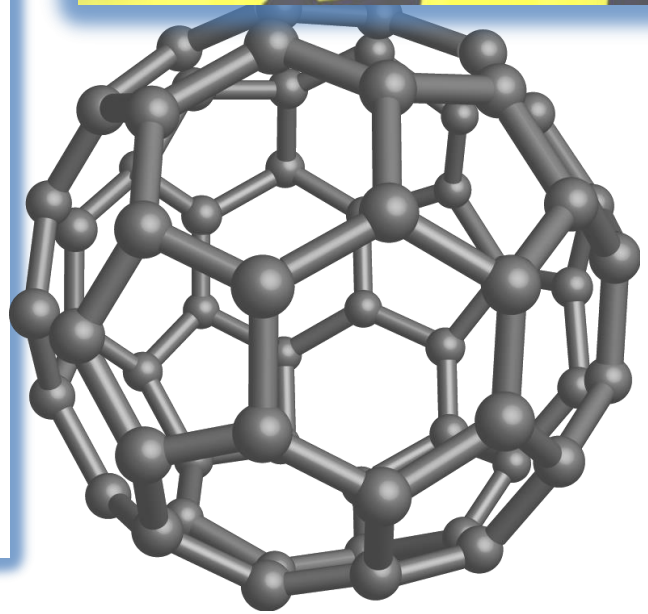

Diffraction: Zeolites

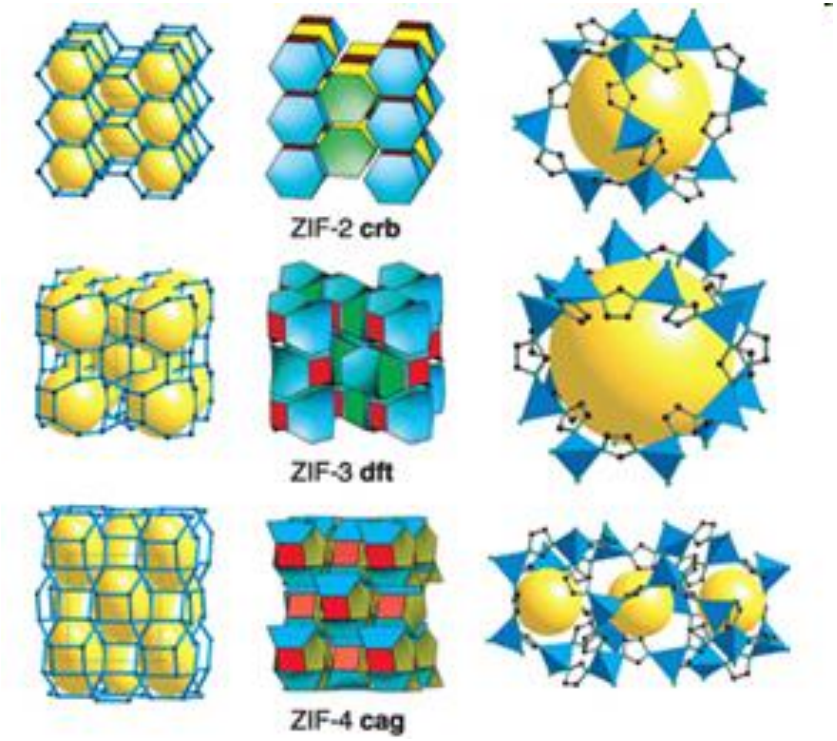

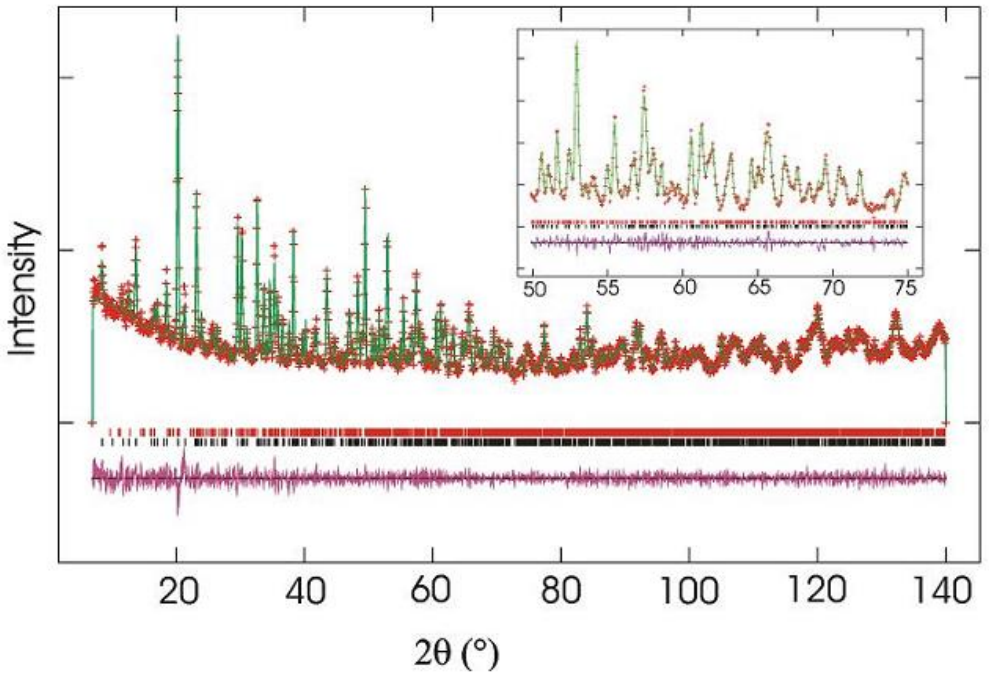

Fig. 1. Observed neutron diffraction intensities (crosses) for deuterium-exchanged RUB-29 superimposed on those computed from the crystallographic model (upper line). The upper and lower sets of short vertical lines indicate reflections of the impurity compound RUB-23 and RUB-29, respectively. The lower curve shows the difference between the observed and calculated data. The plot is enlarged in the high angle range between $50° < 2\theta < 75°$ to emphasize agreement between the data and the model.

Applications:
Detergents: Ion exchange capability
Gas separation: Microporosity
Dessicants: Adsorption
Catalysis: acidity, porosity, high surface area

Large Unit Cell!

Source: B Toby NIST

Batteries

EUROPEAN SPALLATION SOURCE

Experimental vi
diffusion in Li_xFe

SHIN-ICHI NISHIMURA[1], GENKI KOBA
AND ATSUO YAN

[1]Department of Electronic
226-8502, Japan
[2]Institute for Materials Re
[3]Department of Materials
Yokohama 226-8502, Jap
*e-mail: yamada@echem.

Natur

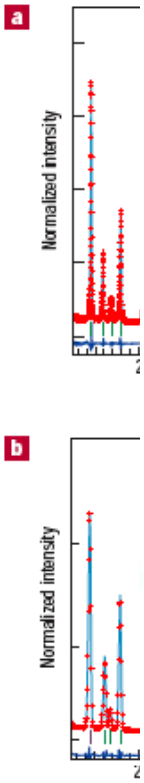

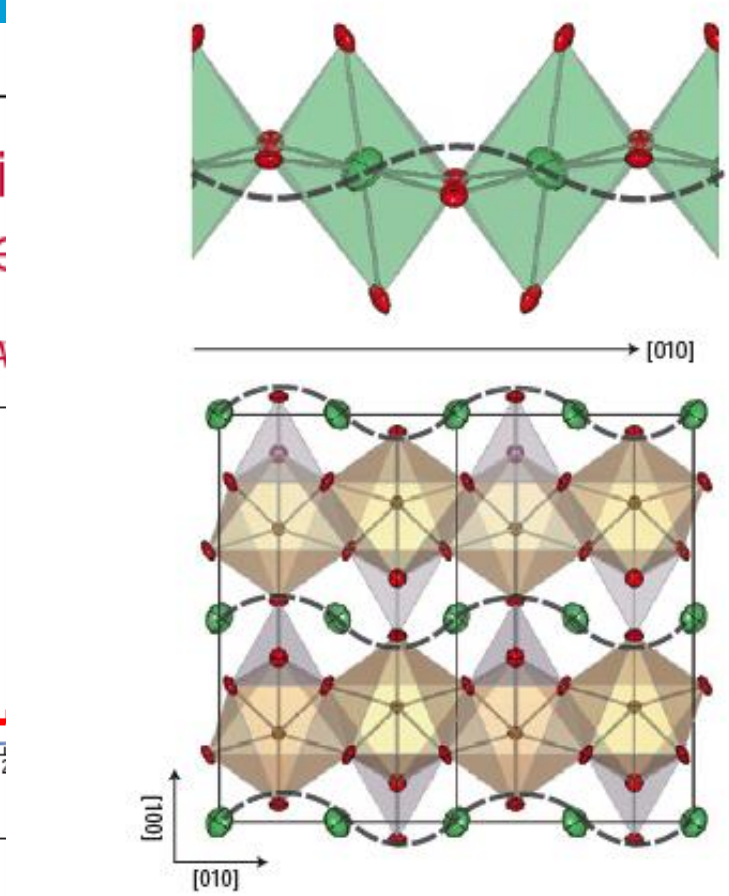

Figure 3 Anisotropic harmonic lithium vibration in $LiFePO_4$ shown as green thermal ellipsoids and the expected diffusion path. The ellipsoids were refined with 95% probability by Rietveld analysis for room-temperature neutron diffraction data. Expected curved one-dimensional continuous chains of lithium motion are drawn as dashed lines to show how the motions of Li atoms evolve from vibrations to diffusion.

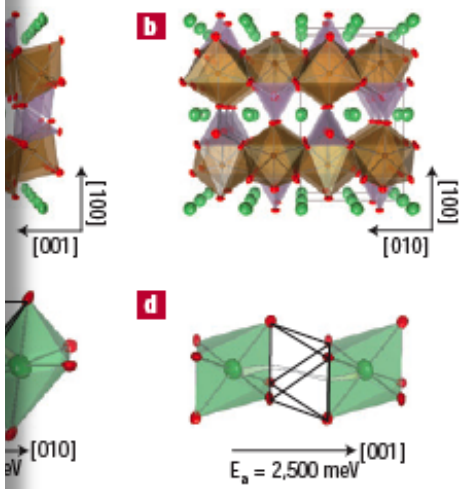

of $LiFePO_4$ and possible lithium pathways. a,b, The projected along the [010] (a) and [001] (b) directions. hways are parallel to these directions. The structures l parameters obtained through this work and ry Information, Table S1. The structure can be agonal close-packed oxygen sub-array, in which Li, Fe ial sites to form (1) corner-sharing FeO_6 octahedra that distorted two-dimensional square lattice perpendicular g LiO_6 octahedra aligned in parallel chains along the $_4$ groups connecting neighbouring planes or arrays. The d ellipsoids indicate Li, Fe, P and O atoms, respectively. e lithium migration paths: **c**, along the [010] direction tetrahedral sites; and **d**, along the [001] direction dral sites. One-dimensional diffusion along the [010] y the computational method[15,16].

Research at Large Facilities

EUROPEAN SPALLATION SOURCE

Laboratory work

Large Scale Facility

Science with Neutrons

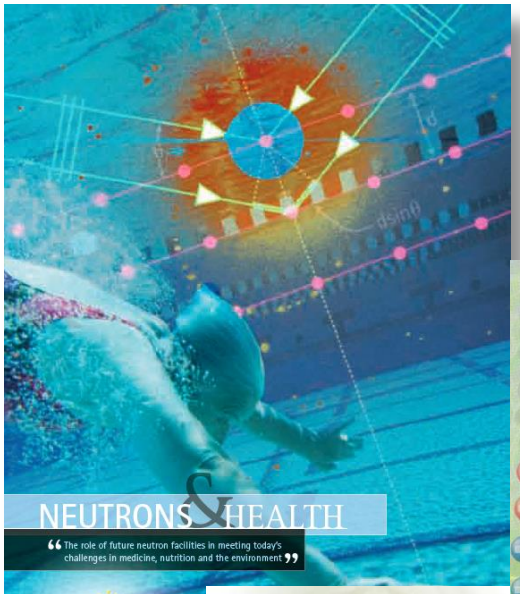

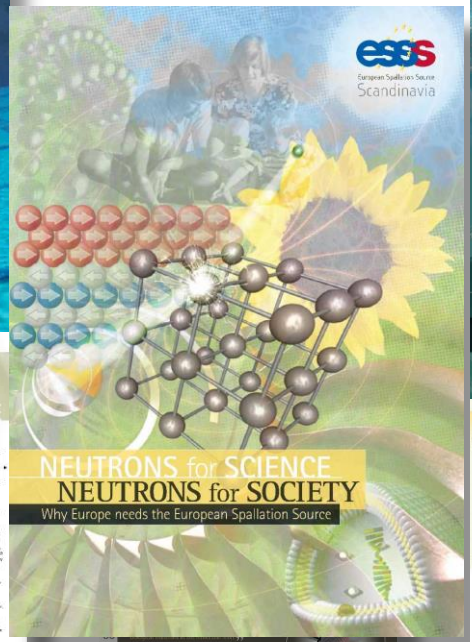

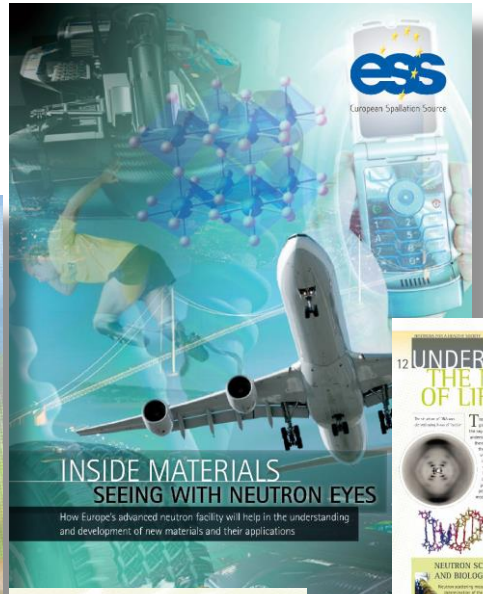

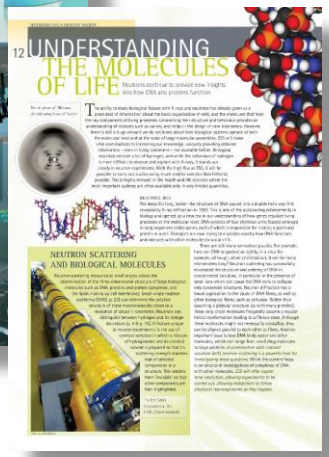

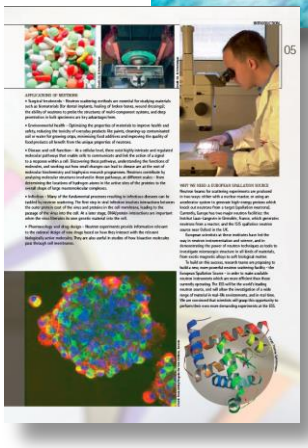

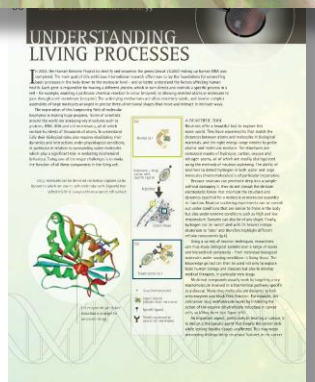

AS

Further Reading

- B.T.M. Willis & C.J. Carlile ‘Experimental Neutron Scattering’, Oxford University Press
- G.L. Squires ‘Introduction to the Theory of Thermal Neutron Scattering’, Cambridge University Press / Dover
- W.I.F. David, K. Shankland, L.B. McCusker, and C. Bärlocher (Eds.) ‘Structure Determination from Powder Diffraction Data‘ IUCr Monographs 13
- Liyuan Liang, Romano Rinaldi, and Helmut Schober, eds, ‘Neutron Applications in Earth, Energy and Environmental Sciences’, ISBN 978-0-387-09415-1, Springer 2009
- A Furrer, J Mesot, T Strässle, ‘Neutron Scattering in Condensed Matter Physics;, World Scientific,
- Google, ISI Web of Science, ScienceDirect..

EXTRA SLIDES

Secondary particle produced at J-PARC

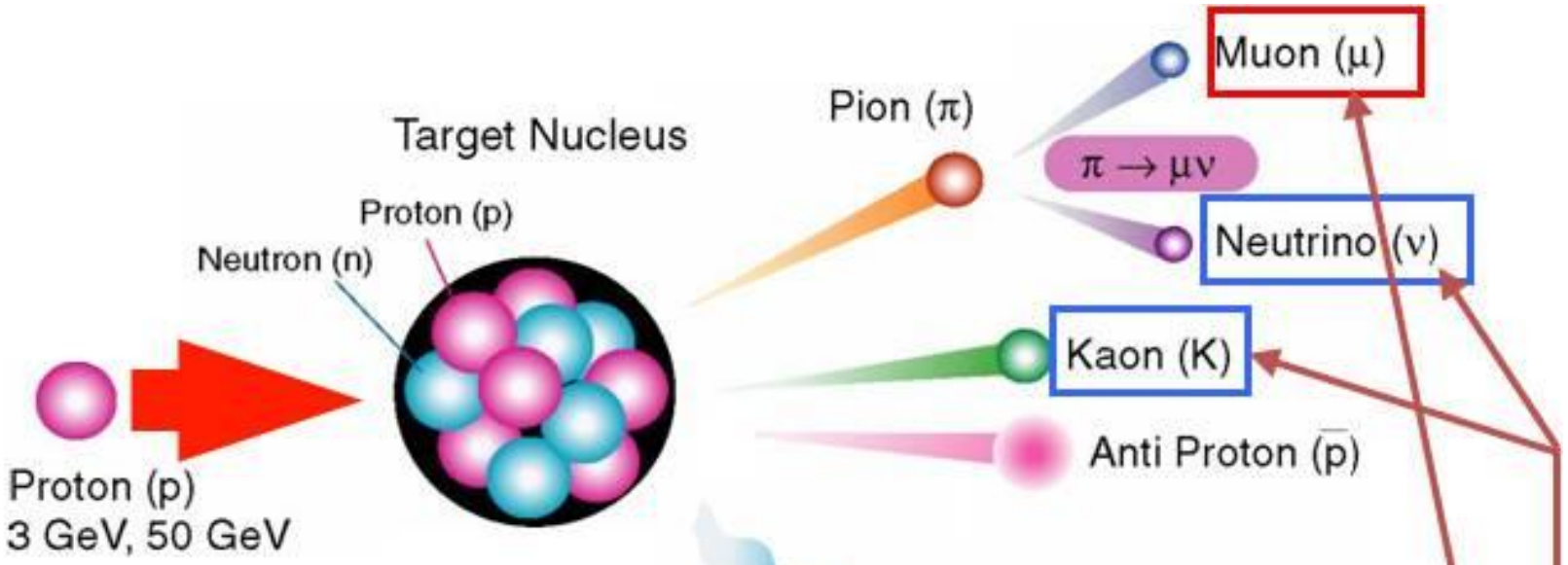

Need to have high-power proton beams

→ MW-class proton accelerator (current frontier is about 0.1 MW)

Materials & Life Science from RCS

Nuclear & Particle Physics from MR

R&D toward Transmutation from LINAC